The VOL-CALPUFF Model for Atmospheric Ash Dispersal: I. Approach and Physical Formulation

S. Barsotti, A. Neri

Istituto Nazionale di Geofisica e Vulcanologia - Sezione di Pisa, Pisa, Italy

J. S. Scire

TRC Companies, Inc., Atmospheric Studies Group, Lowell, Massachusetts,

USA

S. Barsotti, INGV - Sezione di Pisa - Via Della Faggiola 32, 56126 Pisa, Italy

A. Neri, INGV - Sezione di Pisa - Via Della Faggiola 32, 56126 Pisa, Italy

J. S. Scire, Atmospheric Studies Group -TRC Companies, Inc., Lowell, Massachusetts, USA

D R A F T   November 20, 2007, 9:57am   D R A F T

Abstract.   We present a new modeling tool, named VOL-CALPUFF able

to simulate the transient and three-dimensional transport and deposition of

volcanic ash under the action of realistic meteorological and volcanological

conditions throughout eruption duration. The new model derives from the

CALPUFF System, a software program widely-used in environmental ap-

plications of pollutant dispersion, that describes the dispersal process both

in the proximal and distal regions and also in presence of complex orogra-

phy. The main novel feature of the model is its capability of coupling a Eulerian

description of plume rise with a Lagrangian representation of ash dispersal

described as a series of diffusing packets of particles or puffs. The model is

also able to describe the multiparticle nature of the mixture as well as the

tilting effects of the plume due to wind action. The dispersal dynamics and

ash deposition are described by using refined orography-corrected meteoro-

logical data with a spatial resolution up to 1 km or less and a temporal step

of 1 hour. The modeling approach also keeps the execution time to a few minutes

on common PCs, thus making VOL-CALPUFF a possible tool for the pro-

duction of ash dispersal forecasts for hazard assessment. Besides the model

formulation, the paper presents the type of outcomes produced by VOL-CALPUFF,

shows the effect of main model parameters on results, and also anticipates

the fundamental control of atmospheric conditions on the ash dispersal processes.

In the companion paper (*Barsotti and Neri* [2007], this issue) a first thor-

ough application of VOL-CALPUFF to the simulation of a weak plume at

28 Mount Etna (Italy) is presented with the specific aim of comparing model

29 predictions with independent observations.

1. Introduction and Background

Amongst the processes associated with an explosive eruption, ash dispersal is probably the phenomenon occurring on the widest range of spatial and temporal scales. Ash particles can have mostly local and regional effects lasting for a few days, if the volcanic column is contained within the troposphere. On the other hand, larger plumes reaching the stratosphere can have a global impact and drive climatic changes for several years. Ash dispersal and fallout can also represent a major hazard for populations near volcanic centers, producing a serious risk for human and animal health and causing damage to crops, ground infrastructures, and aviation traffic (*Sparks et al.* [1997]; *Sigurdsson et al.* [2000]; *Martì and Ernst* [2005]). Due to such a frequent and wide impact of ash fallout the scientific community has produced, for many years, numerical models aimed at describing the rising phase and movements of volcanic particles in the atmosphere. Modeling volcanic ash dispersal is indeed a complex task. It needs detailed information on the system initial and boundary conditions as the volcanic source and temporal and spatial meteorological variations, as well as on the physics that govern the entire phenomenon. Historically, physical models can be roughly divided into two categories: 1) those aimed at describing the dynamics of the volcanic column, and 2) those focused on the description of pyroclast dispersal in the atmosphere and at the ground. In the following paragraphs the main physical models, developed to date, will be briefly recalled together with their main features.

Volcanic column Regarding this first category, early models adopted a pseudofluid approach in which solid particles and gases are assumed to be in thermal and mechanical

equilibrium thus forming a mixture characterized by a bulk density (*Wilson* [1976]; *Wilson and Walker* [1987]; *Sparks et al.* [1997]). The main features of the rising plume phase were described by solving the conservation equations of mass and momentum for the homogeneous mixture and assuming a steady time-averaged 1-D axisymmetric column. Later on, the equation sets of these so-called "plume-theory" models were integrated by adding the energy conservation equation in different forms (*Woods* [1988]; *Glaze and Baloga* [1996]). Further developments concerned the modeling of thermal disequilibrium (*Woods and Bursik* [1991]), particle fallout from the column (*Woods and Bursik* [1991]; *Ernst et al.* [1996]), and umbrella cloud (*Bursik et al.* [1992b]; *Bonadonna et al.* [1998]) and particle recycling into the eruption column (*Ernst et al.* [1996]; *Veitch and Woods* [2002]; *Veitch and Woods* [2004]; *Textor et al.* [2004]). Crosswind influence on plume tilting has also been addressed based on experimental and theoretical work on turbulent buoyant plumes in cross flow (*Hoult and Weil* [1972]; *Wright* [1984]; *Ernst et al.* [1994]; *Bursik* [2001]). These types of models were also used to obtain simple correlations to estimate column height (*Carey and Sparks* [1986]; *Bursik et al.* [1992a]; *Bonadonna et al.* [1998]). The evaluation of column height is indeed crucial for quantifying the area affected by ash fallout. These correlations link column height with the excess thermal energy associated with the column (*Morton et al.* [1956]; *Morton* [1959]) or directly with the mass flow rate (*Sparks* [1986]; *Sparks et al.* [1997]). Similar dimensional arguments are used to estimate column height in a windy environment (*Wright* [1984]). The dynamics of buoyant volcanic columns have also been recently investigated by adopting transient, multidimensional, and multiphase flow models able to describe new features of the phenomenon. For instance, the ATHAM code (*Oberhuber et al.* [1998]; *Herzog et al.* [1998]; *Graf et al.* [1999]; *Textor et al.* [2004];

74 *Textor et al.* [2006a]; *Textor et al.* [2006b]) is a fully 3D non-hydrostatic limited area

75 circulation model able to describe the eruption column behavior, including accurate cloud

76 physics and microphysical processes, on spatial scales of a few hundred kilometers and

77 up to few hours of eruption time. Similarly, *Dartevelle et al.* [2004] recently analyzed the

78 2D transient behavior of buoyant volcanic clouds of different scales by using a two-phase

79 mixture description. The influence of the third dimension and turbulence closure has been

80 discussed by *Suzuki et al.* [2005] by using a pseudogas approximation of the multiphase

81 mixture.

82 **Pyroclastic dispersal and deposition** With respect to this second category of models,

83 first attempts were by *Suzuki* [1983], *Armienti et al.* [1988], *Macedonio et al.* [1988], *Mace-*

84 *donio et al.* [1990] and, more recently, by *Macedonio et al.* [2005] and *Costa et al.* [2006],

85 who adopted advection-diffusion equations and solved them in 2D and 3D domains. Other

86 studies based on this approach discuss the effect of various parameterizations of the source

87 and the production of probabilistic hazard maps (*Bonadonna et al.* [2002]; *Bonadonna*

88 *et al.* [2005]; *Pfeiffer et al.* [2005]). In these models the volcanic column is parameterized

89 by an empirical source function and particles diffuse under the action of constant winds.

90 An alternative approach, mostly used to reproduce the deposit features, assumes the wind-

91 advected volcanic material to be spreading radially as an intrusive gravity current above

92 the level of neutral buoyancy (*Sparks et al.* [1991]; *Bursik et al.* [1992b]; *Bonadonna et al.*

93 [1998]). Models based on alternative approaches have also been developed by different

94 groups. The PUFF model (*Searcy et al.* [1998]) describes the movements of a collection of

95 discrete ash particles representing a sample of the eruption cloud by using a Lagrangian

96 scheme and treating the source as a virtual pre-assigned vertical distribution of mass.

97 Similarly, the HYSPLIT code (*Draxler and Taylor* [1982]; *Draxler and Hess* [1998]) de-

98 scribes, by means of a Lagrangian approach, the evolution of puffs (containing material

99 particles with diameters up to 30 μm) without taking account of buoyancy effects. Other

100 codes are in use at the Volcanic Ash Advisory Centers (VAACs). CANERM (*Simpson*

101 *et al.* [2002]) (operative at the Canadian Meteorological Center), is a 3D Eulerian model

102 used for medium- and long-range transport which assumes a virtual source described by

103 a vertical mass distribution. Similarly, MEDIA (*Piedelievre et al.* [1990]) (operative at

104 Toulouse Meteo France), is a Eulerian atmospheric transport/diffusion model focused on

105 long-range dispersal of particles ejected from a source at a given altitude. NAME (*Watkin*

106 *et al.* [2004]) (operative at the UK Met Office), is a Lagrangian particle model that can

107 be applied on either regional or global scales and is able to consider areal as well as point-

108 like sources. Finally, VAFTAD (*Heffter and Stunder* [1993]) (developed by NOAA ARL

109 and in use at the Washington and Anchorage VAACs), is a 3D time-dependent Eulerian

110 model which needs the maximum height reached by the volcanic column to model the

111 input source. Currently all the above models are of limited value for volcanic ash disper-

112 sal forecasting, despite being used at VAACs, in that they all lack a source-term matrix

113 derived from an understanding of basic eruption physics (GGJ. Ernst, pers. communica-

114 tion). This realization is one of the key motivations for developing the present work.

115

2. Aim of the Work

116 From the above summary it is clear that the dynamics of the rising volcanic plume and of

117 the dispersal and depositional processes have been mostly treated separately despite their

118 being part of the same phenomenon and being strictly inter-related. Moreover, volcanic

plume models typically cannot be applied under realistic meteorological conditions and, similarly, dispersal models do not account for realistic source conditions as they adopt what may appear as subjective parameterization of the source. Finally, most of the dispersal models in use at research and operative centers are relevant only to medium- and long-distance areas, whereas the importance of forecasting the ash dispersal also in proximal regions is crucial for nearby inhabited areas and aviation routes. In this case a treatment of meteorological datasets able to include effects on wind fields due to the presence of complex orography is also necessary. The aim of this work is to present a new modeling system, named VOL-CALPUFF, able to simulate the transient and three-dimensional injection, transport and deposition of volcanic ash under the action of realistic and unperturbed meteorological and volcanological conditions. The main novel feature of the model is its capability of coupling a Eulerian plume rise model with a Lagrangian representation of ash dispersal described as a series of diffusing packets of particles or "puffs". Like several other codes used in volcanological applications, VOL-CALPUFF has its origin in an air quality modeling code named CALPUFF designed for the transport of pollutants at local and long-distance scales (*Nguyen et al.* [1997]; *Scire et al.* [2000]). The VOL-CALPUFF code differs from the original CALPUFF code in several aspects fully described in this paper, which makes it suitable for volcanological applications. The main differences include the implementation of a multiparticle plume model, the possibility of treating particles larger than a few microns, the consideration of puff dispersal well above the atmospheric boundary layer, and the consideration of various settling velocity laws as a function of particle size and shape. It is also worth noting that the VOL-CALPUFF code can describe the whole dispersal dynamics and deposition by using very refined orography-

corrected meteorological data - with a final resolution up to 1 km or less - while keeping

the execution time in the order of minutes on common PCs. All these features also make

VOL-CALPUFF a promising tool for the production of ash dispersal forecasts for hazard

assessment. In the following sections an overview of the CALPUFF System, the main

features of the new VOL-CALPUFF code, and some sensitivity tests for weak plumes,

will be presented. The companion paper (*Barsotti and Neri* [2007], this issue) will present

a first complete application of the new code to a weak plume of Mt. Etna.

3. An Overview of the CALPUFF System

With the term "CALPUFF System" we mean the whole numerical procedure that from

meteorological and geophysical input data computes hourly the concentration of released

material, gaseous or particulate, in the atmosphere and at the ground. The CALPUFF

system was developed by Earth Tech Inc. (now TRC Companies, Inc.) in the 1990s

and it is freely available on line at the website http://www.src.com/calpuff/calpuff1.htm.

CALPUFF is a quite complex model composed of a great number of sub-processors linked

to each other by an input-output data flow. It has a modular structure, so that, depending

on the available input data and type of information required, the model elaboration can

follow different patterns. Fig. 1 shows a simplified basic configuration of the system such

as the one we have used in our study. The procedure starts with the elaboration of the

geophysical information, such as terrain elevation and land-use data, once the choice of

the computational domain under investigation is made. In parallel with the elaboration

of the geophysical information, processing of the meteorological data occurs to provide

CALMET (see hereafter) with the necessary input data. The meteorological processor

CALMET is a diagnostic code; this means that it computes the values of meteorological

164 variables on a finer grid without solving the time-dependent equation of motion. CALMET

165 works in two steps that refine and correct an initial guess field typically provided by a

166 prognostic code (e.g. MM5, ETA). In the first step the initial data are interpolated on a

167 grid usually much finer than that used in mesoscale models, and the local orography effects

168 are accounted for (*Scire et al.* [1990]; *Scire and Robe* [1997]). In the second step, surface

169 or upper air data, when available, are considered to correct the computed wind field

170 through an objective analysis that assigns appropriate weight to each data. The output

171 provided by CALMET contains the 3D fields (such as wind and temperature) and the 2D

172 field of micro-meteorological variables (like friction velocity, Obukhov length, atmospheric

173 boundary layer height and Pasquill-Gifford-Turner stability classes). All these variables

174 are computed with the temporal resolution required by the dispersal model and on a

175 grid in a terrain-following coordinate system with a vertical and horizontal user-defined

176 resolution. This file, together with that containing the data related to the volcanic source,

177 is fed as input to the system's core, i.e. the CALPUFF dispersal model.

178 The CALPUFF code describes atmospheric ascent and dispersion of a gaseous mixture

179 under the action of advective, turbulent wind fields. The rising plume phase is computed

180 in a Eulerian way by solving the plume theory equation, whereas dispersal is described

181 in a Lagrangian framework. In particular, assuming a hot gaseous mixture, CALPUFF

182 reproduces the plume up to its maximum height, corresponding to a null vertical velocity.

183 At this altitude continuous material emission is discretized in several packets (the *puffs*),

184 so that at each time-step a finite number of puffs are released. The mass flow rate

185 associated with the puffs matches the mass flow rate computed at the top of the rising

186 plume. Each puff is associated with a given particle size and release time. The number of

187 puffs is mainly determined by the wind speed at the source and is computed to adequately

188 represent a continuous release. The wind present at the altitude at which the puffs are

189 injected causes the puff center to move in the horizontal direction, whereas the settling

190 velocity, also acting on the puff center, brings the puffs towards the ground. During the

191 displacement the material inside the puff is affected by vertical and horizontal diffusion,

192 which causes the puff to spread. Under the assumption of Gaussian packets, their diffusion

193 is described by lateral and vertical standard deviations. Finally, it is worth noting that the

194 CALPUFF System has been validated through extensive comparison of model predictions

195 with experimental data such as the Cross-Appalachian Tracer Experiment (CAPTEX).

196 The CAPTEX experiment involved the release of a unique series of tracers for the purpose

197 of providing data to evaluate and improve computer models of pollutant dispersion and to

198 provide insight into the mechanisms of long-range transport and dispersion. To compare

199 CALPUFF to other widely used codes, further studies (Kincaid and Lovett data set) were

200 conducted; these studies suggest that the CALPUFF dispersion model allows appropriate

201 characterization of both local-scale and long-range transport and dispersion (*EPA U.S.*

202 [1998d]; *Earth Tech, Inc.* [2002]). Due to the model performance, the U.S. Environmental

203 Protection Agency (*EPA U.S.* [1998a]; *EPA U.S.* [1998b]; *EPA U.S.* [1998c]; *Irwin* [1998];

204 *Scire et al.* [2000]) proposed CALPUFF as a guideline model for regulatory applications

205 involving long-range transport and near-field applications where non-steady-state effects

206 may be important.

4. The VOL-CALPUFF Code

207 Fig. 2 illustrates the main features of the VOL-CALPUFF code we developed in the

208 present work. In the following sub-sections, the main equations and features of the new

model will be described by highlighting the main developments carried out with respect
to the original CALPUFF code.

4.1. Meteorological Pre-processors

The need to describe dispersal under the forcing of realistic meteorological conditions
makes the treatment of the original weather forecasting data a crucial step. The flow-
chart reported in Fig. 1 shows the presence of two different meteorological pre-processors
needed to provide VOL-CALPUFF with the required meteorological information. The
first, CALITA, is aimed at decoding and rewriting, in a format readable by CALMET,
the data produced in grib (GRIdded Binary, see *Stackpole* [1994]) format by the mesoscale
prognostic code. CALITA is optimized for working on meteorological data coming from
different sources as those produced by the Italian Lokal Modell (COSMO's web-site
[2004]). CALITA can also use meteorological data coming from the Reanalysis Archive of
the European Center for Medium-Range Weather Forecast (ECMWF) and National Cen-
ters for Environmental Prediction (NCEP-NOAA) in such a way that they can be read
by CALMET. Using CALITA it is possible to define the subdomain being investigated
and the number of atmospheric levels the user is interested in. It provides CALMET with
3D fields of pressure (and related geopotential height), temperature, wind direction, wind
speed, pressure vertical velocity and relative humidity, together with 2D field of pressure at
sea level, total rainfall accumulation and snow cover indicator. The second pre-processor,
CALMET, is a diagnostic model able to produce a quite simplified analysis of the at-
mosphere by describing either mesoscale dynamics or micrometeorological processes. The
latter includes an energy budget model for the computation of appropriate boundary layer
scaling parameters such as surface heat flux, surface momentum flux and boundary layer

231 height, which are used to derive the friction velocity, the convective velocity scale and the

232 Monin-Obukhov length (*Scire et al.* [1990]). In this study, we run CALMET in a "non-

233 observational" mode, i.e. without including assimilation of meteorological data coming

234 from weather stations, using mesoscale output files as an initial guess field. The spatial

235 resolution adopted is 1 km and applies to the entire computational domain.

4.2. Rising Plume Phase

236 This part of the VOL-CALPUFF code is new since the built-in plume rise model al-

237 ready implemented in CALPUFF was able to treat only gaseous emissions with a density

238 lower than atmospheric. Therefore a more general plume rise model was implemented in

239 VOL-CALPUFF to take into account the presence of a number of solid particulate phases.

240 The equation set was solved in a 2D Cartesian coordinate system (s, φ) by considering

241 the bulk properties of the eruptive mixture (see Fig. 2). The plume is assumed with

242 a circular section along the curvilinear coordinate s and an inclination on the ground

243 defined by an angle φ between the axial direction and the horizon. This last feature is

244 needed to describe the evolution of weak explosive eruptions which are strongly affected

245 by atmospheric conditions.

246 As in the plume theory, the entrainment (due to both turbulence in the rising buoyant

247 jet and to the crosswind field) is parameterized through the use of two entrainment co-

248 efficients, α and γ. The theory assumes that the efficiency of mixing with ambient air is

249 proportional to the product of a reference velocity (the vertical plume velocity in one case

250 and the wind field component along the plume centerline in the other), α and γ (*Morton*

251 [1959]; *Briggs* [1975]; *Wright* [1984]; *Weil* [1988]). Although this simplified approach can

252 be used to reproduce the first-order features of plume ascent (e.g. final plume height), it

does not explicitly describe more complex observed dynamics such as the double-vortex structure (*Ernst et al.* [1994]). The equation set consists of the equations of conservation of mass, momentum and thermal energy for the bulk mixture with height, equations expressing the conservation of mass for pyroclasts of different sizes, and those describing the variation of specific heat and mixture gas constant. The equation system is completed by the perfect gas law for the gaseous phase by assuming equilibrium pressure conditions between the volcanic plume and surrounding atmosphere. The total mass conservation equation solved by the model is:

$$\frac{d(\beta U_{sc}r^2)}{ds} = 2r\rho_a[\alpha|U_{sc} - U_a cos\varphi| + \gamma|U_a sin\varphi|] + $$
$$-p\beta r(1-n)\sum_{i=1}^{N}w_s(i)y_i \tag{1}$$

The variation of mass flux (l.h.s. term) is due to air entrainment and loss of solid particles (first and second r.h.s. terms, respectively). In Eq. (1), U_{sc} represents the velocity of the plume cross-section along its centerline, r the plume radius, β the mixture bulk density and U_a is the horizontal wind speed. This equation is similar to that used by *Bursik* [2001], the only difference being the lack of the re-entrainment term, which we assume to be negligible for the low intensity bent-over plumes discussed below and in the companion paper (*Ernst et al.* [1996]; *Bursik* [2001]). The factor p reflects, from a geometrical point of view, the possibility of each particle falling out from the rising plume and, by assuming clasts are lost only from the sloping plume margins, it is a function of the radial entrainment coefficient only (*Bursik et al.* [1992a]):

$$p = \frac{2((1 + \frac{6}{5}\alpha)^2 - 1)}{(1 + \frac{6}{5}\alpha)^2 + 1} \tag{2}$$

275 For our values of α, the p factor varies between 0.2 and 0.33 (α=0.09 and α=0.15, re-

276 spectively). The influence of the two entrainment coefficients, α and γ, was investigated

277 through sensitivity studies (see next section), but in most cases they were set to 0.09 and

278 0.6, respectively, as determined in experimental studies by *Morton et al.* [1956], *Briggs*

279 [1975] and *Weil* [1988]. As shown in the companion paper (*Barsotti and Neri* [2007],

280 this issue), these values for the two coefficients can provide quite consistent estimates of

281 plume height and deposit accumulation for the 2001 Etna plume investigated. In Eq. (1),

282 the quantities $w_s(i)$ and y_i are the settling velocity and mass fraction, respectively, of the

283 i-th granulometric class. The term in which they appear is the contribution of particle

284 sedimentation from the plume.

285 Defining n as the mass fraction of the gaseous phase, the term $\pi\beta U_{sc}r^2(1-n)y_i$ represents

286 the mass flux in the plume of the i-th particulate class. To compute the variation of the

287 mass flux of solids during ascent the model solves the N mass conservation equations for

288 the N particulate phases; which result in:

$$\frac{d(\beta U_{sc}r^2(1-n)y_i)}{ds} = -pw_s(i)\beta r(1-n)y_i \qquad i = 1,...,N. \tag{3}$$

290 The X- and Z-components of the momentum balance solved by the model are:

$$\frac{d(\beta U_{sc}r^2(u-U_a))}{ds} = -r^2\beta w\frac{dU_a}{dz} - up\beta r(1-n)\sum_{i=1}^{N}w_s(i)y_i \tag{4}$$

$$\frac{d(\beta U_{sc}r^2 w)}{ds} = gr^2(\rho_a-\beta) - wp\beta r(1-n)\sum_{i=1}^{N}w_s(i)y_i \tag{5}$$

294 where the two components of plume velocity along the X and Z axes are u and w,

295 respectively, and are linked by the relation $U_{sc} = \sqrt{u^2+w^2}$. In the r.h.s. of Eq. (4) appear

296 the terms related to the exchange of momentum due to the wind and to momentum loss

297 from the fall of solid particles. Similar contributions are evident in the r.h.s. term of Eq.

298 (5) where the vertical momentum is changed by the gravitational acceleration term and

299 the segregation of particles.

300 Finally, following the above adopted notation, the equation for conservation of thermal

301 energy solved by VOL-CALPUFF is described as:

302 $$\frac{d(\beta U_{sc} r^2 C_{p_{mix}} T_p)}{ds} = 2r\rho_a C_a T_a(\alpha|U_{sc} - U_a cos\varphi + \gamma|U_a sin\varphi|) +$$

303 $$-r^2 w \rho_a g +$$

304 $$-T_p p \beta r(1-n) * \sum_{i=1}^{N} C_s(i)w_s(i)y_i \qquad (6)$$

305   The first term on r.h.s. describes the cooling of the plume due to ambient air entrain-

306 ment, the second one takes into account atmospheric thermal stratification, and the third

307 term allows for heat loss due to sedimentation of solid particles. A thermal equilibrium

308 between solid and gaseous phases is assumed. This formulation is similar to that proposed

309 by *Glaze and Baloga* [1996] adapted for a two-dimensional and multi-phase treatment.

310 Finally, two equations for the variation rate of mixture specific heat and for the mixture

311 gas constant were derived. Both variables were defined as weighted averages on the mass

312 fraction of the components. We report the expression for the gas constant only, obtained

313 knowing that the variation of gaseous mass fraction with height is solely due to entrained

314 air:

315

316 $$\frac{dR_g}{ds} = \frac{n_0 \beta_0 U_{sc_0} r_0^2 (R_{air} - R_{gv})}{n^2 \beta^2 U_{sc}^2 r^3} * 2\rho_a[\alpha|U_{sc} - U_a cos\varphi| + \gamma|U_a sin\varphi|] \qquad (7)$$

317   where R_{gv} is the gas constant for the specific volcanic gas component. This formulation

318 reduces, for particular cases, to the expressions of *Woods* [1988] and *Glaze and Baloga*

319 [1996]. The plume rise equations were solved with a predictor-corrector Heun's scheme

320 that guarantees a second-order accuracy, keeping the execution time in the order of sec-

321 onds. Vent boundary conditions include the initial plume radius (r_0), mixture velocity

322 (U_{sc_0}) and temperature (T_0), gas mass fraction (n_0) and the physical properties of the

323 granulometric population.

4.3. Puff Transport and Diffusion

324 The mass flow rate feeding the puffs corresponds to the particle flow rate feeding the

325 plume at the vent corrected for the amount radially lost during ascent. VOL-CALPUFF

326 then describes pyroclast transport and diffusion in the atmosphere by tracking the move-

327 ments of a number of Gaussian puffs, calculating their position, their lateral and vertical

328 diffusion, and their amount of mass. Puff center displacement is computed by the simple

329 relation $\overline{S} = \overline{V} * t$. Horizontally, the puff center is subjected to vertically-averaged zonal

330 and meridional winds ($\overline{V}_H = \sqrt{U_{ave}^2 + V_{ave}^2}$), whereas vertically it is subjected only to the

331 fall velocity ($\overline{V}_V = V_{set}$). The vertical component of the wind field is indirectly accounted

332 for through a vertical spreading of the puff obtained by varying the vertical dispersion

333 coefficient as a function of the vertical velocity gradient (*Scire et al.* [2000]). During puff

334 movement, the mass distribution of a given particle size within the puff changes due to

335 turbulent phenomena. Puff concentration is described by a Gaussian distribution whose

336 standard deviations, horizontal and vertical, are computed for each time step. For a

337 circular puff, the mathematical expression of such a distribution, which also represents

338 the puff contribution to the concentration computed at a given location (*receptor*), is the

339 following:

340

$$C(s) \;=\; \frac{Q(s)}{2\pi\sigma_y^2} g_t e^{\frac{-R^2(s)}{(2\sigma_y^2)}} \tag{8}$$

342

$$g_t \;=\; \frac{1}{(2\pi)^{\frac{1}{2}}\sigma_z} \sum_{n=-\infty}^{\infty} [e^{\frac{-(z_r - H_e + 2nh)^2}{(2\sigma_z^2)}} + e^{\frac{-(z_r + H_e + 2nh)^2}{(2\sigma_z^2)}}] \tag{9}$$

where s is the distance traveled by the puff from the source, $R(s)$ is the horizontal distance between puff center and receptor, and g_t is the vertical term, also called the coupling term, which depends on the puff and receptor relative positions. In particular, in case of puffs below the atmospheric boundary layer the coupling term takes into account, through the infinite sum over the index n, the material entrapment between the ground and the mixing lid of thickness h. Puff mass is represented by the variable Q and it varies with time by material removal due to sedimentation. Finally, the sigmas represent the horizontal and vertical diffusions. Their formulation is expressed as follows:

$$\sigma_{y,n}^2 = \sigma_{yt}^2 + \sigma_{ys}^2 + \sigma_{yb}^2 \tag{10}$$

$$\sigma_{z,n}^2 = \sigma_{zt}^2 + \sigma_{zb}^2 \tag{11}$$

where the horizontal term (Eq. (10)) contains the contribution due to atmospheric turbulence (σ_{yt}), the contribution due to a lateral (cross-wind) scale of the vent area-source (σ_{ys}) and the contribution due to plume buoyancy at the time of release (σ_{yb}). A similar formulation is valid for the vertical term (Eq. (11)), where the contribution due to areal extension is missing. These expressions show how the model allows the puffs to spread not only in response to atmospheric turbulence (σ_{yt} and σ_{zt}), but also in relation to the dynamics of the plume and to its structure when reaching the maximum

363 rise height. In particular, the puffs are characterized by lateral dispersal coefficients

364 (σ_{yb} and σ_{zb}) which are a function of the plume top radius. Furthermore the sigmas

365 ($\sigma_{y,n}$ and $\sigma_{z,n}$) are functions of travel time (from source to receptor) and are computed

366 each time the puff has a non-null contribution to the receptor. Finally, it should be

367 noted that, in contrast to CALPUFF, the VOL-CALPUFF code is able not only to track

368 the transport of puffs well above the atmospheric boundary layer (which can vary from

369 hundreds of meters to a few kilometers above the ground), but also to compute their

370 concentrations at the receptor locations. This extension of the code is indeed necessary

371 due both to the much greater heights reached by volcanic plumes with respect to emission

372 from industrial stacks and to our interest in mapping ash concentration anywhere, i.e. not

373 only on the ground. Additional features implemented in VOL-CALPUFF are related to

374 the consideration of particles with different diameters (up to several millimeters) and to

375 the effect of particle shape on their settling velocity. With respect to the first aspect, VOL-

376 CALPUFF can represent the multisize nature of the eruptive mixture by considering, at

377 each time step, different independent puffs, each one characterized by a specific particle

378 diameter. This is possible due to the dilute nature of the dispersal system that makes

379 the interaction between particles negligible (*Crowe et al.* [1998]). Regarding the second

380 aspect, several past and recent studies have highlighted the importance of describing

381 the effect of particle sizes (*Bonadonna et al.* [1998]) as well as non-sphericity on their

382 falling velocities (*Walker* [1971]; *Wilson* [1972]; *Wilson and Huang* [1979]; *Riley et al.*

383 [2003]; *Dellino et al.* [2005]). The original CALPUFF code restricts the computation of

384 settling velocity to the atmospheric layer affected by default activities and, as default,

385 uses Stokes's formulation for spherical particles. VOL-CALPUFF adopts a formulation of

the settling velocity as function of the Reynolds number. In particular, it adopts Stoke's

drag coefficient expression C_D=24/Rey for Reynolds numbers smaller than $Rey < 0.1$ and

$C_D \sim 1$ for $Rey > 1000$ (*Walker* [1971]). For Reynolds numbers in the 0.1-100 range, the

Wilson and Huang formulation is used (*Wilson and Huang* [1979]). The latter formulation

appears to be a good trade-off between ease of formulation and accuracy of results. It

defines the following relationship between the drag coefficient, C_D, and Reynolds number

:

$$C_D = \frac{24}{Rey}F^{-0.28} + 2\sqrt{1.07 - F} \tag{12}$$

in which particle shape affects the factor F through the equation $F = \frac{b+c}{2a}$, where

a, b, and c are the three principal axes of the particle. Lastly, for intermediate values

$100 < Rey < 1000$ a linear interpolation between the above described correlations is

assumed for C_D (as already suggested by *Pfeiffer et al.* [2005]). The settling velocity of

non-spherical particles is also allowed to vary as a function of height above the ground due

to major variations in air density and viscosity with altitude (*Wilson* [1972]). In contrast,

particle aggregation processes are not described by the present model, although they can

play a major role in some conditions (*Textor and Ernst* [2004]; *Veitch and Woods* [2004]).

5. Initial Analyzes and Model Outputs

In this section first applications of the VOL-CALPUFF will be presented to show some

of its standard outputs and type of results it is able to provide. In particular, the plume

model was applied to the investigation of some interactions between plume rise and disper-

sal processes and the atmospheric environment, in the case of weak explosive events. Mete-

407 orological data used were produced by the non-hydrostatic EURO-LM Model (COSMO's

408 web-site [2004]).

409 **Plume dynamics** Several simulations were performed by varying the conditions of the

410 eruptive mixture at the vent in a still vs. windy environment. The results obtained were

411 plotted in terms of variations of column density, velocity, and temperature with height

412 and also compared to previous models (*Woods* [1988]; *Bursik and Woods* [1991]; *Bursik*

413 [2001]). As an example, keeping constant the meteorological data and the vent velocity,

414 and increasing vent radius, the model reproduced the shift in eruptive style from buoyant

415 to super-buoyant and then to collapsing plumes, already predicted for plumes rising in a

416 still atmosphere (*Bursik and Woods* [1991]). But the novel feature of VOL-CALPUFF is

417 its ability to describe the effect of horizontal wind field on column evolution. As illustrated

418 in the companion paper (*Barsotti and Neri* [2007], this issue), this is an important new

419 feature of the code that strongly affects dispersal and deposition processes. This effect

420 is shown in Fig. 3 where the column height evolution with time is reported for a still

421 (thin line) and windy environment (bold one), for two intensities and for two seasonal

422 periods. Even for constant vent feeding, weather conditions can modify column height by

423 up to 100% or more. The sensitivity of plume dynamics to wind action is shown for an

424 intensity range typical of weak explosive eruptions. In the absence of wind, the influence

425 of atmospheric stratification on column height can also be inferred by comparing the tem-

426 poral column evolutions in different seasonal periods (summer vs. winter). During colder

427 periods, for both intensities, the plume reaches slightly greater heights in the atmosphere

428 (*Wilson and Walker* [1987]).

429 The effect of the wind field on plume tilting can be seen in Fig. 4. The figure reports

two different wind speed profiles (bold lines) and the associated distances reached by the column axis along the vertical and downwind directions. In particular, Fig. 4a shows the plume response to the tilting effect of wind for two real meteorological conditions, in the early morning and at midday, for a mass flow rate of $6.6 * 10^3$ kg/s. Similarly, Fig. 4b shows the results for a higher plume intensity ($2.5 * 10^4$ kg/s). The investigated wind profiles produce quite different plume rise trajectories. From the figure it is evident how the plume, meeting the more intense wind, rises about 25 % less high than that affected by the weaker winds; whereas the downwind distance of the plume top is only slightly sensitive.

VOL-CALPUFF can also be used to assess the sensitivity of results to the model parameters, for instance to the entrainment coefficients. Fig. 5a and Fig. 5b show the variation of column height, calculated each hour during a 72-hour run with constant vent conditions, as a function of the two entrainment coefficients. The figure clearly shows the irregular trends which reflect the temporal variability of meteorological conditions met by the column during ascent. However, the role of the entrainment coefficients (Eq. 1) in the determination of column height is also evident. Keeping the wind-entrainment coefficient γ equal to 0.6, the radial-entrainment coefficient α was varied in the range 0.09-0.15 (Fig. 5a). The first value was proposed by *Morton et al.* [1956] and is typically assumed for buoyant volcanic plumes (*Sparks et al.* [1997]). The second value comes from laboratory experiments (*Hewett et al.* [1971]). In agreement with *Morton et al.* [1956] and *Wilson and Walker* [1987], increasing the radial coefficient, α, the column reaches decreasing altitudes. The VOL-CALPUFF results show that, in a windy environment, this variation is reflected in an approximately 30% change of column height.

453 A similar sensitivity study was performed for a variation of γ in the range 0.6-1.0 (derived

454 by *Briggs* [1975] and *Hewett et al.* [1971], respectively), confirming the inverse relation be-

455 tween column height and entrainment coefficient. The two simulations, keeping α equal

456 to 0.09, show a stronger dependence on wind-entrainment variation, which produces a

457 difference of up to about 40% in column height (Fig. 5b).

458 **Ash dispersal** In addition to the analysis of plume evolution, VOL-CALPUFF provides

459 consistent estimates of atmospheric ash concentrations and particle deposition at the

460 ground. Each hour it computes the quantity of emitted material still airborne and the

461 amount deposited. In our standard applications the domain is sliced into eight terrain-

462 following levels at 800 m intervals with each one made up of 5625 points. Both the

463 number of levels as well as the gridded points can be increased. Particle concentration

464 is computed at each receptor. Fig. 6 shows a vertical section of the domain used in the

465 application at Mt. Etna (discussed in the companion paper), in which levels have been

466 remapped referring to sea level. The horizontal levels are parallel planes in which the color

467 is graduated depending on the amount of computed ash. More intuitive is a planar view

468 representation where the contouring of particle concentration (g/m^3), at a specific altitude

469 above the ground, is superimposed on a 2D topography (Fig. 7). The code's Lagrangian

470 nature and the algorithms's structure make it easy to quantify the presence of ash in

471 specific locations and at any height of interest, for example in correspondence of airplane

472 flight levels or corresponding to areas with anthropogenic activities. Ash concentration

473 estimates at plume levels may prove valuable to fine tune remote-sensing instruments as

474 regards particle diameter and density, as well as, detection thresholds. Finally, at the

475 ground level, VOL-CALPUFF can compute the dry-fluxes of depositing material from

which the ash load is estimated in kg/m^2. A 3D representation of this output is provided by Fig. 8, in which the computed deposit is *spread* on a 3D orographic profile.

6. Conclusive Remarks

The VOL-CALPUFF model is a new quantitative tool for simulating atmospheric dispersal and deposition of volcanic ashes. The main new feature of the model is its ability to combine plume rise and ash dispersal models to describe their dynamics under the action of realistic 3D and time-dependent meteorological conditions. The model, by adopting a mixed Eulerian-Lagrangian formulation, is able to describe effectively the rising column and regional ash dispersal throughout the eruption. The Lagrangian description of ash dispersal provides a reliable model both in the distal and proximal areas. Moreover, spatial and temporal resolution scales in the order of 1 km and 1 hour, respectively, can be provided by VOL-CALPUFF by keeping the computational time to a few minutes even for eruptive events lasting several days. This feature makes VOL-CALPUFF a promising tool also for the production of quasi real-time ash dispersal forecast simulations to be used for warning and hazard analysis (*Barsotti et al.* [2006]). Results from initial simulations clearly highlight the novel features of the model and the important implications that they allow regarding dispersal dynamics. With specific reference to the rising plume dynamics, the results presented show the extensive influence of meteorological conditions on plume height. The wind speed variations during the three-day period investigated result in the plume height variations of well above 100%. An increase in wind speed by a few meters per second at low altitude can significantly tilt the rising plume, shifting the plume top several hundreds of meters closer to the ground (see Fig. 4). In absence of wind, the column height also shows sensitivity to the variations of atmospheric thermal stratification.

498 In the companion paper (*Barsotti and Neri* [2007], this issue) VOL-CALPUFF is used to

499 model a weak plume from Mt. Etna, and results are compared to independent observa-

500 tions to better describe VOL-CALPUFF capabilities and limitations. Model applications

501 to larger plumes are being prepared and will be presented in future works.

Notation

a	major mean particle axes
b	median mean particle axes
c	minor mean particle axes
$C_{p_{mix}}$	heat capacity of mixture
C_a	heat capacity of ambient air
C_D	drag coefficient
C_s	heat capacity of solid phase
$C(s)$	concentration at receptor
F	particle shape factor
g_t	coupling vertical term
H_e	effective puff height
h	mixing layer height
n	gas mass fraction
n_0	initial gas mass fraction
p	probability of fallout
$Q(s)$	amount of material in each puff
r	plume radius
r_0	initial plume radius
R_{gv}	gas constant for volcanic gas component
R_g	gas constant for mixture gas phase
R_{air}	gas constant of ambient air
Rey	Reynolds's number
s	downstream coordinate or source-puff distance
$\overline{S}$	generic puff displacement
t	time
T_a	ambient temperature
T_p	plume temperature
T_0	initial mixture temperature
U_{ave}	zonal wind averaged over lateral puff extension
U_{sc}	centerline plume velocity
U_{sc_0}	initial centerline plume velocity
U_a	wind speed
V_{ave}	meridional wind averaged over lateral puff extension
V_{set}	settling velocity
$\overline{V}$	generic velocity (both horizontal and vertical) driving puff displacement
$\overline{V}_H$	horizontal puff velocity
$\overline{V}_V$	vertical puff velocity
$w_s(i)$	settling velocity of i-th granulometric class
y_i	mass fraction of i-th granulometric class
z_r	receptor height

Notation

α	radial entrainment coefficient
β	mixture bulk density
β_0	initial mixture bulk density
γ	wind-entrainment coefficient
φ	angle between plume axis and horizon
ρ_a	air ambient density
$\sigma_{y,n}$	lateral dispersion coefficient at n time step
σ_{yb}	lateral dispersion coefficient due to plume buoyancy
σ_{ys}	lateral dispersion coefficient due to lateral scale of an area-source
σ_{yt}	lateral dispersion coefficient due to atmospheric turbulence
$\sigma_{z,n}$	vertical dispersion coefficient at n time step
σ_{zb}	vertical dispersion coefficient due to plume buoyancy
σ_{zt}	vertical dispersion coefficient due to atmospheric turbulence

References

Armienti, P., G. Macedonio, and M.T. Pareschi (1988), A numerical-model for simulation of tephra transport and deposition - applications to May 18, 1980, Mount-St-Helens eruption, *J. Geophys. Res., 93* , 6463–6476.

Barsotti, S. and A. Neri (2007), The VOL-CALPUFF model for atmospheric ash dispersal: II. Application to the Weak Mt. Etna Plume of July 2001, submitted to *J. Geophys. Res.*.

Barsotti, S., L. Nannipieri and A. Neri (2006), An early-warning system for volcanic ash dispersal: The MAFALDA procedure, Abstract no. V21C-06 AGU Fall Meeting, San Francisco, CA, 11-15 December 2006.

Bonadonna, C., G. G. J. Ernst and R. S. J. Sparks (1998), Thickness variations and volume estimates of tephra fall deposits: The importance of particle Reynolds number, *J. Volcanol. Geotherm. Res. 81*, 173-187.

Bonadonna, C., G. Macedonio and R. S. J. Sparks (2002), Numerical modelling of tephra fallout associated with dome collapses and Vulcanian explosions: Application to haz-

ard assessment on Montserrat, in *The eruption of Soufrire Hills Volcano, Montserrat, from 1995 to 1999, Geological Society Memoir*, no.21, edited by T.H. Druitt and B.P. Kokelaar, pp. 517–537, Geological Society of London, Bath, UK.

Bonadonna, C., C. B. Connor, B. F. Houghton, L. Connor, M. Byrne, A. Laing and T. K. Hincks (2005), Probabilistic modeling tephra dispersal: Hazard assessment to a multiphase rhyolitic eruption at Tarawera, New Zealand, *J. Geophys. Res.*, *110*, B03203, doi:10.1029/2003JB002896.

Briggs, G. A. (1975), Plume rise predictions, in *Lectures on air pollution and environmental impact analyses*, edited by Duane A. Hangen, pp. 59–111, American Meteorological Society, Boston, MA.

Bursik, M. I. (2001), Effect of wind on the rise height of volcanic plumes, *Geophys. Res. Lett., 28*, 3621–3624.

Bursik, M. I. and A. W. Woods (1991), Buoyant, superbuoyant and collapsing eruption columns, *J. Volcanol. Geotherm. Res., 45*, 347–350.

Bursik, M. I., R. S. J. Sparks, S. N. Carey and J. S. Gilbert (1992a), Sedimentation of tephra by volcanic plumes: I Theory and its comparison with a study of the Fogo A plinian deposit, Sao Miguel (Azores), *Bull. Volcanol., 54*, 329–344.

Bursik, M. I., S. N.Carey and R. S. J. Sparks (1992b), A gravity current model for the May 18, 1980 Mount St. Helens plume, *Geophys. Res. Lett., 19*, 1663–1666.

Carey, S. N. and R. S. J. Sparks (1986), Quantitative models of the fallout and dispersal of tephra from volcanic eruption columns, *Bull. Volcanol., 48*, 109–125.

Costa, A., G. Macedonio and A. Folch (2006), A three-dimensional Eulerian model for transport and deposition of volcanic ashes, *Earth and Science Planetary Letters, 241*,

546 634–647.

547 Consortium for Small-scale Modeling (COSMO)'s web-site: http://cosmo-model.cscs.ch/

548 Crowe, C., M. Sommerfeld and Y. Tsuji (1998), Multiphase flows with droplets and par-

549 ticles, CRC Press, Boca Raton, Florida.

550 Dartevelle, S., W. I. Rose, J. Stix, K. Kelfoun and J. W. Vallance (2004), Numerical

551 modeling of geophysical granular flows: 2. Computer simulations of Plinian clouds

552 and pyroclastic flows and surges, *Geochemistry Geophysics Geosystem*, *5*, Q08004, doi:

553 10.1029/2003GC000637.

554 Dellino, P., D. Mele, R. Bonasia, G. Braia, L. La Volpe and R. Sulpizio (2005), The

555 analysis of the influence of pumice shape on its terminal velocity, *Geophys. Res. Lett.*,

556 *32*, L21306, doi:10.1029/2005GL023954.

557 Draxler, R. R. and A. D. Taylor (1982), Horizontal dispersion parameters for long-range

558 transport modelling, *J. Appl. Met.*, *21*, 367–372.

559 Draxler, R. R. and G. D. Hess (1998), An overview of the HYSPLIT_4 modelling system

560 for trajectories, dispersion and deposition, *Austral. Meteorol. Mag.*, *47*, 295–308.

561 Earth Tech, Inc. (2002), Application of CALMET/CALPUFF and MESOPUFF II to

562 compare regulatory design concentrations for a typical long-range transport analysis,

563 U. S. EPA Report, Earth Tech, 196 Baker Avenue, Concord, Massachusettes 01742.

564 Environmental Protection Agency U.S. (1998a), A comparison of CALPUFF modelling

565 results to two tracer field experiment, EPA-454/R-98-009, Office of Air Quality Planning

566 and Standards, U. S. EPA, Research Triangle Park, NC 27711.

567 Environmental Protection Agency U.S. (1998b), An analysis of the CALMET/CALPUFF

568 modeling system in a screening mode, EPA-454/R-98-010, Office of Air Quality Planning

and Standards, U. S. EPA, Research Triangle Park, NC 27711.

Environmental Protection Agency U.S. (1998c), A comparison of CALMET/CALPUFF with ISC3, EPA-454/R-98-020, Office of Air Quality Planning and Standards, U. S. EPA, Research Triangle Park, NC 27711.

Environmental Protection Agency U.S. (1998d), Interagency Workgroup on air quality modelling (IWAQM) Phase2: Summary report and recommendations for modelling long range transport impacts, EPA-454/R-98-019, Office of Air Quality Planning and Standards, U. S. EPA, Research Triangle Park, NC 27711.

Ernst, G. G. J., J. P. Davis and R. S. J. Sparks (1994), Bifurcation of volcanic plumes in crosswind, *Bull. Volcanol.*, *56*, 159–169.

Ernst, G. G. J., R. S. J. Sparks, S. N. Carey and M.I. Bursik (1996), Sedimentation from turbulent jets and plumes, *J. Geophys. Res.*, *101*, 5575–5589.

Glaze, L. S. and S. M. Baloga (1996), Sensitivity of buoyant plume heights to ambient atmospheric conditions: Implications for volcanic eruption columns, *J. Geophys. Res.*, *101*, 1529–1540.

Graf, H. F., M. Herzog, J. M. Oberhuber and C. Textor (1999), Effect of environmental conditions on volcanic plume rise, *J. Geophys. Res.*, *104*, 24309–24320.

Heffter, J. L. and B. J. B. Stunder (1993), Volcanic ash forecasting transport and dispersion (VAFTAD) model, *Weath. Forecast.*, *8*, 533–541.

Herzog, M., H-F. Graf, C. Textor and J. M. Oberhuber (1998), The effect of phase changes of water on the development of volcanic plumes, *J. Volcanol. Geotherm. Res.*, *87*, 55–74.

Hewett, T. A., J. A. Fay and D. P. Hoult (1971), Laboratory experiments of smokestack plumes in a stable atmosphere, *Atmos. Environ.*, *5*, 769–789.

Hoult, D. P. and J. C. Weil (1972), A turbulent plume in laminar crossflow, *Atmos. Environ.*, *6*, 513–531.

Irwin, J. S. (1998), Interagency Workgroup on Air Quality Modeling (IWAQM) Phase2: Summary report and recommendations for modeling long range transport impacts, EPA-454/R-98-019, Office of Air Quality Planning and Standrds, U.S.EPA, Research Triangle Park, NC.

Macedonio, G., M.T. Pareschi, and R. Santacroce (1988), A numerical simulation of the Plinian fall phase of 79 AD eruption of Vesuvius, *J. Geophys. Res.*, *93*, 14817–14827.

Macedonio, G., M.T. Pareschi, and R. Santacroce (1990), Renewal of explosive activity at Vesuvius: Models for the expected tephra fallout, *J. Volcanol. Geotherm. Res.*, *40*, 327–342.

Macedonio, G., A. Costa and A. Longo (2005), A computer model for volcanic ash fallout and assessment of subsequent hazard, *Computer & Geosciences*, *31*, 837–845.

Martì, J. and G. G. J. Ernst (eds. 2005), Volcanoes and the Environment, Cambridge University Press, Cambridge, UK.

Morton, B. R. (1959), Forced plumes, *J. Fluid Mech.*, *5*, 151–163.

Morton, B. R., F. R. S. Taylor and J. S. Turner (1956), Turbulent gravitational convection from maintained and instantaneous sources, *Proceedings of the Royal Society of London*, *234*, 1–23.

Nguyen, K. C., J. A. Noonan, I. E. Galbally and W. L. Physick (1997), Predictions of plume dispersion in complex terrain: Eulerian versus Lagrangian models, *Atmos. Environ.*, *31*, 947–958.

614   Oberhuber, J. M., M. Herzog, H. F. Graf and K. Schwanke (1998), Volcanic plume simu-

615   lation on large scales, *J. Volcanol. Geotherm. Res.*, *87*, 29–53.

616   Pfeiffer, T., A. Costa and G. Macedonio (2005), A model for the numerical simulation of

617   tephra fall deposits, *J. Volcanol. Geotherm. Res.*, *140*, 273–294.

618   Piedelievre, J. P., L. Musson-Genon and F. Bompay (1990), MEDIA - An Eulerian model

619   of atmospheric dispersion: a first validation on the Chernobyl release, *J. Appl. Meteor.*,

620   *29*, 1205–1220.

621   Riley, C. M., W. I. Rose and G. J. S. Bluth (2003), Quantitative shape measurements of

622   distal volcanic ash, *J. Geophys. Res.*, *108*, 2504, doi:10.1029/2001JB000818.

623   Scire, J. S., E. M. Insley and R. J. Yamartino (1990), Model formulation and user's guide

624   for the CALMET meteorological model, Report, Sigma Research Corp., Concord, MA,

625   USA.

626   Scire, J. S. and F. R. Robe (1997), Fine scale application of the CALMET meteorological

627   model to a complex terrain site, Air&Waste Management Association's 90th Annual

628   Meeting & Exhibition, Toronto, Ontario, Canada, June 8-13.

629   Scire, J. S., D. G. Strimaitis and R. J. Yamartino (2000), CALPUFF User's guide, avail-

630   able at http://www.src.com/calpuff/download/download.htm

631   Searcy, C., K. Dean and W. Stringer (1998), PUFF: A Lagrangian trajectory volcanic ash

632   tracking model, *J. Volcanol. Geotherm. Res.*, *80*, 1–16.

633   Sigurdsson, H., B. Houghton, H. Rymer, J. Stix and S. McNutt (2000), *Encyclopedia of*

634   *volcanoes*, Academic Press, San Diego, CA.

635   Simpson, J. J., G. L. Hufford, R. Servranckx, J. S. Berg and C. Bauer (2002), The

636   February 2001 eruption of Mt.Cleveland, Alaska: Case study of an aviation hazard,

637   *American Meteor. Soc.*, *17*, 691–704.

638   Sparks, R. S. J. (1986), The dimensions and dynamics of volcanic eruption columns, *Bull.*

639   *Volcanol.*, *41*, 1–9.

640   Sparks, R. S. J., S. N. Carey and H. Sigurdsson (1991), Sedimentation from gravity

641   currents generated by turbulent plumes, *Sedimentology, 38*, 839–856.

642   Sparks, R. S. J., M. I. Bursik, S. N. Carey, J. S. Gilbert, L. S. Glaze, H. Sigurdsson and

643   A. W. Woods (1997), *Volcanic plumes*, J. Wiley, New York.

644   Stackpole, J. D. (1994), A guide to GRIB (Edition 1) The WMO format for the storage of

645   weather product information and the exchange of weather product messages in gridded

646   binary form, Automation Division, National Meteorological Center, National Weather

647   service, NOAA.

648   Suzuki, T. (1983), A theoretical model for dispersion tephra, in *Arc volcanism: Physics*

649   *and Tectonics*, edited by Shimozuru D. and I. Yokoyama, 93–113, Terra Scientific Pub-

650   lishing Company, Tokyo.

651   Suzuki, Y. J., T. Koyaguchi, M. Ogawa and I. Hachisu (2005), A numerical study of

652   turbulent behaviour in eruption clouds using a three dimensional fluid-dynamics model,

653   *J. Geophys. Res., 110*, B08201, doi:10.1029/2004JB003460.

654   Textor, C. and G. G. J. Ernst (2004), Comment on "Particle aggregation in volcanic

655   eruption columns" by Graham Veitch and Andrew W. Woods, *J. Geophys. Res.*, *109*

656   (B5), B05202, doi:10.1029/2002JB002291.

657   Textor, C., G. G. J. Ernst, M. Herzog and A. Tupper (2004), Potential of the ATHAM

658   model for Use in air traffic safety, Proceedings of 2nd International Conference on

659   Volcanic Ash and Aviation Safety, VAAS, pp. 15–19, OFCM, Alexandria, Virginia,

660 USA, June 21-24.

661 Textor, C., H. F. Graf, M. Herzog, J. M. Oberhuber, W. I. Rose and G. G. J. Ernst (2006a),

662 Volcanic particle aggregation in explosive eruption columns. Part I: Parameterization of

663 the microphysics of hydrometeors and ash, *J. Volcanol. Geotherm. Res.*, *150*, 359–377.

664 Textor, C., H. F. Graf, M. Herzog, J. M. Oberhuber, W. I. Rose and G. G. J. Ernst

665 (2006b), Volcanic particle aggregation in explosive eruption columns. Part II: Numerical

666 experiments, *J. Volcanol. Geotherm. Res.*, *150*, 378–394.

667 Veitch, G. and A. W. Woods (2002), Particle recycling in volcanic plumes, *Bull. Volcanol.*,

668 *64*, 31–39.

669 Veitch, G. and A. W. Woods (2004), Reply to comment by C. Textor and G. G. J. Ernst on

670 particle aggregation in volcanic eruption columns, *J. Geophys. Res. 109* , (B5), B05203,

671 doi:10.1029/2003JB002388.

672 Walker, G. P. L. (1971), Grain-size characteristics of pyroclastic deposits, *J. Geol.*, *79*,

673 696–714.

674 Watkin, S., S. Karlsdòttir, N. Gait, D. Ryall and H. Watkin (2004), Volcanic ash monitor-

675 ing and forecasting at the London VAAC, Proceedings of 2nd International Conference

676 on Volcanic Ash and Aviation Safety, VAAS, pp. 65–69, OFCM, Alexandria, Virginia,

677 USA, June 21-24.

678 Weil, J. C. (1988), Plume rise, in *Lectures on air pollution modelling*, Editors Venkatram

679 A. and Wyngaard J. C., 119–166

680 Wilson, L. (1972), Explosive volcanic eruptions II. The atmospheric trajectories of pyro-

681 clast, *Geophys. J. R. astr. Soc.*, *30*, 381–392.

Wilson, L. (1976), Explosive volcanic eruptions III. Plinian eruption columns, *Geophys. J. R. astr. Soc*, *45*, 543–556.

Wilson, L. and T. C. Huang (1979), The influence of shape on the atmospheric settling velocity of volcanic ash particles, *Earth and Planetary Science Letters*, *44*, 311–324.

Wilson, L. and G. P. Walker (1987), Explosive volcanic eruptions VI. Ejecta dispersal in plinian eruptions: the control eruption conditions and atmospheric properties, *Geophys. J. R. astr. Soc*, *89*, 657–679.

Woods, A. W. (1988), The fluid dynamics and thermodynamics of eruption columns, *Bull. Volcanol.*, *50*, 169–193.

Woods, A. W. and M. I. Bursik (1991), Particle fallout, thermal disequilibrium and volcanic plumes, *Bull. Volcanol.*, *53*, 559–570.

Wright, S. J. (1984), Buoyant jets in density-stratified crossflow, *J. Hydr. Eng.*, *110*, 5, 643–656.
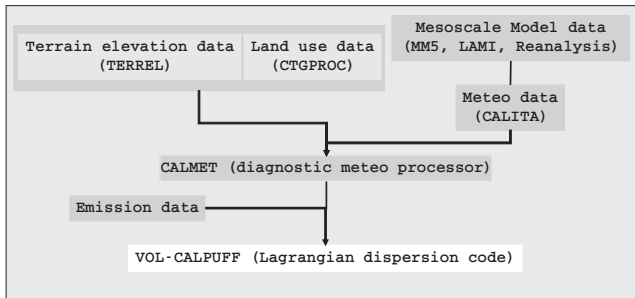
Figure 1.   The simplified flowchart of CALPUFF as used in our application. It represents the minimal structure for running the system. It contains the meteorological and geophysical preprocessors (TERREL, CTGPROC, CALITA), the diagnostic meteorological model (CALMET), and the dispersal code (VOL-CALPUFF).
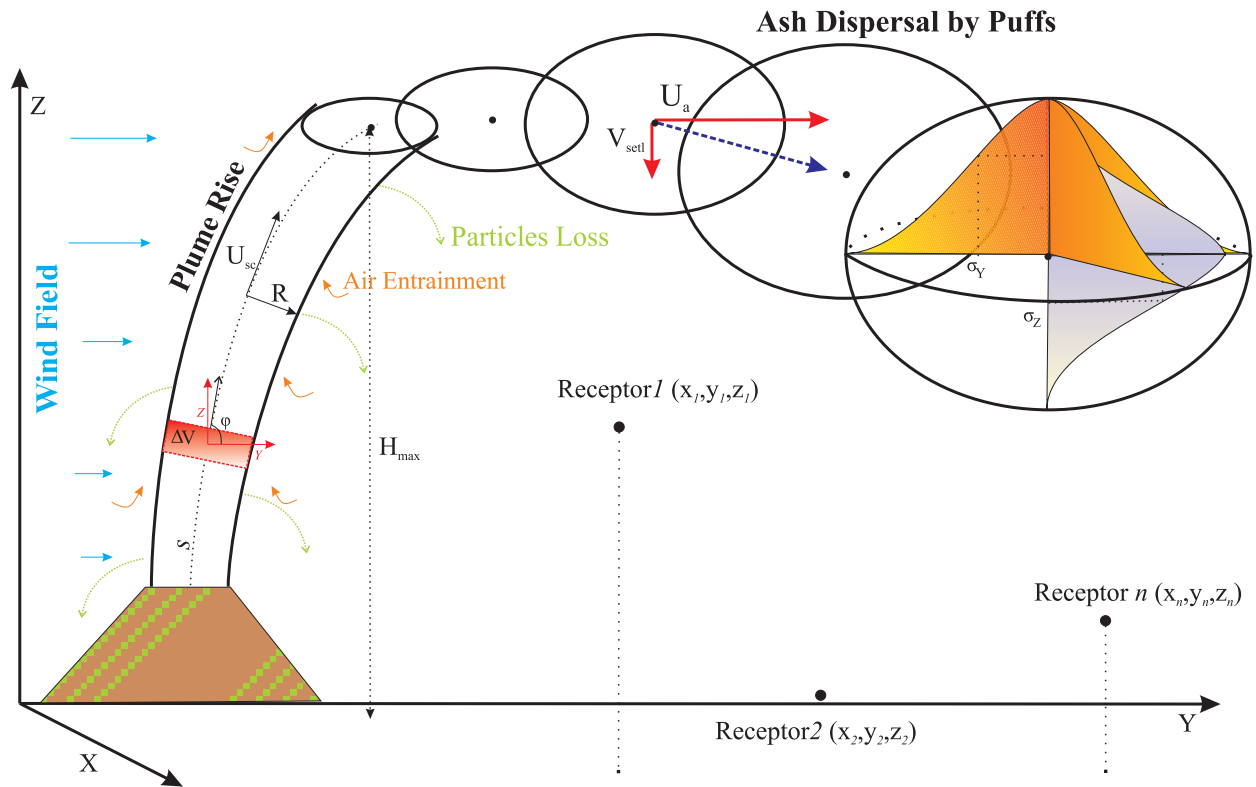
Figure 2. Schematic representation of the VOL-CALPUFF approach. Plume ascent is described by adopting a Eulerian formulation whereas dispersal is represented by a Lagrangian approach, i.e. following the movement and diffusion of a discrete number of puffs.
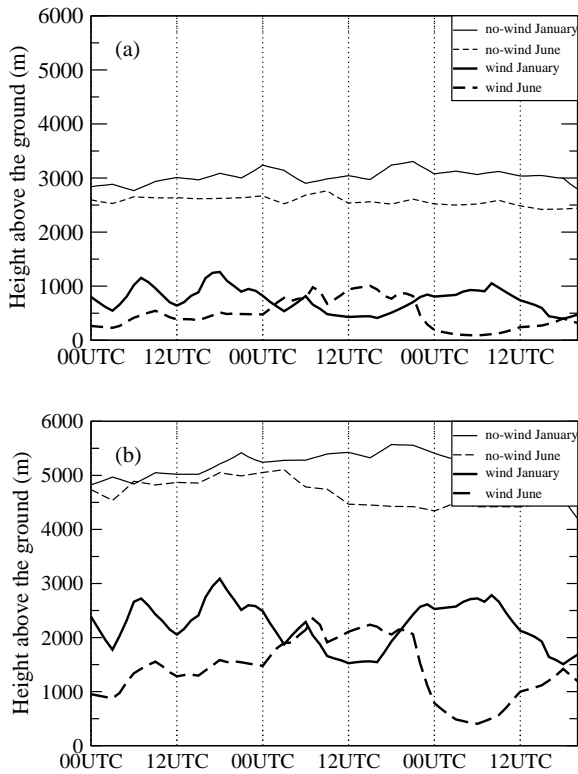
Figure 3.   Variation of column height for two plume intensities, (a) $6.6 * 10^3$ kg/s (T_0=1300 K, U_{sc_0}=20 m/s, r_0=4.8 m, n_0=3%) and (b) $2.5*10^4$ kg/s (T_0=1300 K, U_{sc_0}=25 m/s, r_0=8.7 m, n_0=3%). Curves refer to a still (thin line) and windy (bold line) atmosphere, and to two different seasonal periods. In detail dashed lines refer to three days of June 2005 whereas the continuous ones indicate three days of January 2006.
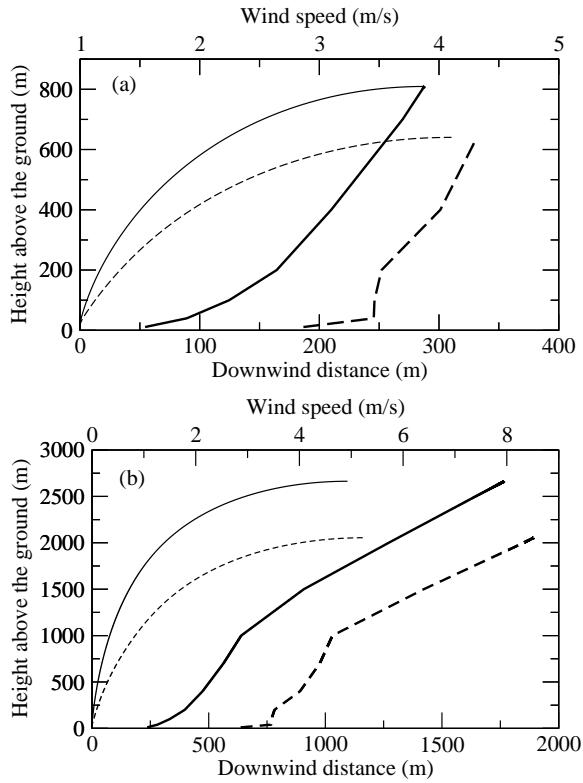
Figure 4.   Effect of wind field on plume height and tilting for two different plume

intensities and meteorological conditions. The intensities correspond to (a) $6.6 * 10^3$ kg/s

and (b) $2.5 * 10^4$ kg/s and vent conditions are the same as Fig. 3. Wind profiles refer to

0600UTC and 1300UTC on 4 January 2006. From the figure it is clear how more intense

speeds (dashed line) tilt the columns more than in the weaker cases (continuous line),
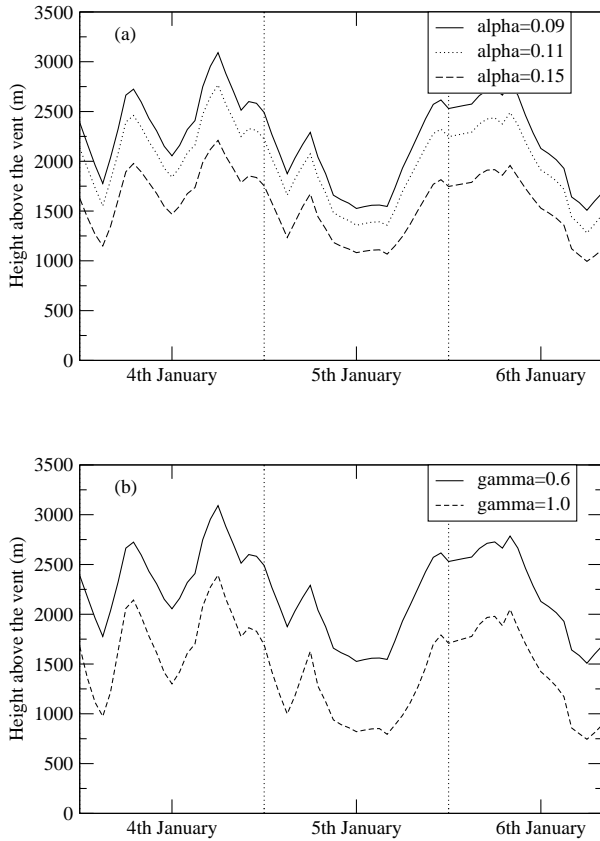
reaching lower heights.

Figure 5. Temporal variations of column height for a mass-flow rate equal to $2.5 * 10^4$ kg/s (the vent conditions are the same as Fig.3). The figures report the height trend over about three days (4-6 January 2006) under the forcing of realistic 3D meteorological conditions. The curves were obtained using different entrainment coefficient values. Keeping γ=0.6 three values of α are investigated (a): $\alpha = 0.11$ (dotted line), $\alpha = 0.15$ (dashed line) and α= 0.09 (continuous line). And, keeping α=0.09, two values of γ (b): $\gamma = 0.6$ (continuous line) and γ=1.0 (dashed line).
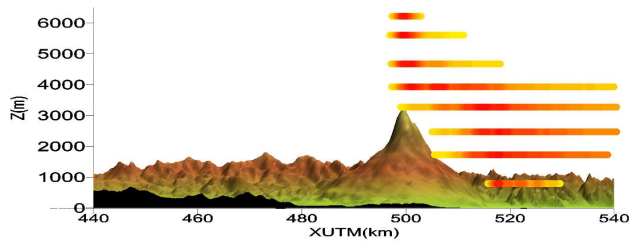
Figure 6. Vertical section of the 3D physical domain in which the horizontally extended levels, remapped from the standard terrain-following ones, are visible. In this case, VOL-CALPUFF adopted eight levels each one made up of 5625 nodes.
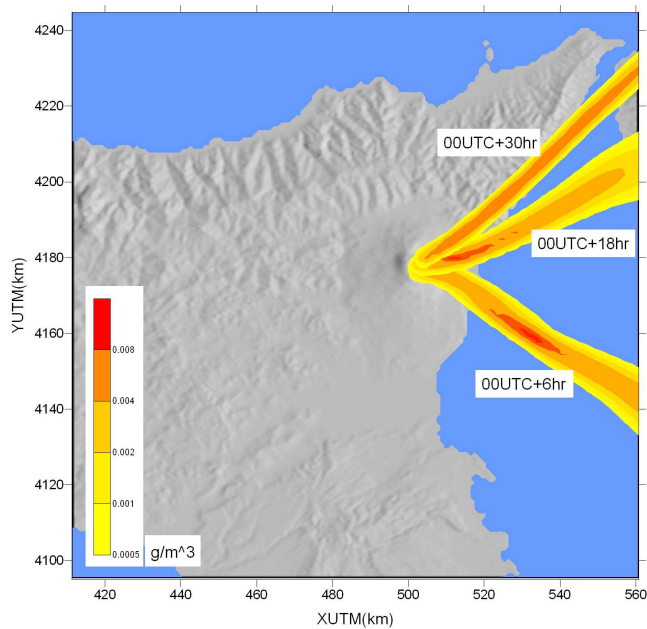

Figure 7. Contouring of 64μm particles concentration at 2400 m a.g.l. in a 2D representation of the VOL-CALPUFF outputs. The three snapshots correspond to three temporal instants at 12hr intervals. Variations in wind direction deflect the plume from SE to a NE dispersal.
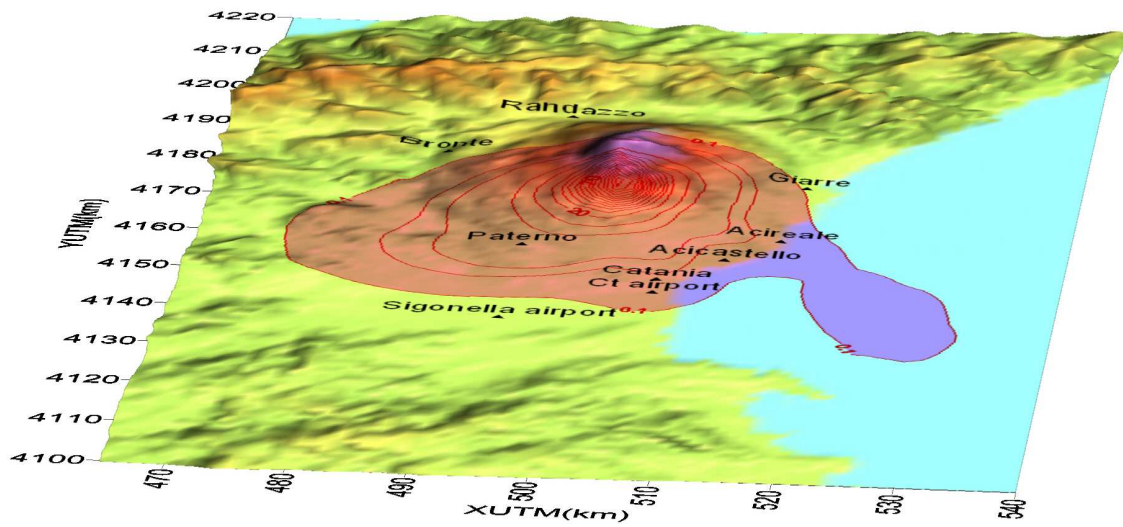
Figure 8.   A given example of deposit on the ground at Mt.Etna. VOL-CALPUFF computes the deposited ash amount in kg/m^2; the lower reported value is equal to 0.1.